

Current Biology

Sleep Disturbance Forecasts β -Amyloid Accumulation across Subsequent Years

Highlights

- Impaired sleep is associated with a higher rate of future β -amyloid accumulation
- Slow-wave activity and sleep efficiency both forecast this increase in β -amyloid
- Sleep may serve as a marker of future Alzheimer's disease risk and the speed of progression

Authors

Joseph R. Winer, Bryce A. Mander, Samika Kumar, Mark Reed, Suzanne L. Baker, William J. Jagust, Matthew P. Walker

Correspondence

mpwalker@berkeley.edu

In Brief

Winer et al. demonstrate that objective measures of sleep physiology forecast subsequent β -amyloid accumulation in healthy older adults. Reduced slow-wave activity and low sleep efficiency at baseline are both associated with accelerated rate of cortical β -amyloid plaque deposition.

Report

Sleep Disturbance Forecasts β -Amyloid Accumulation across Subsequent Years

Joseph R. Winer,¹ Bryce A. Mander,² Samika Kumar,¹ Mark Reed,¹ Suzanne L. Baker,³ William J. Jagust,^{3,4} and Matthew P. Walker^{1,4,5,*}

¹Center for Human Sleep Science, Department of Psychology, University of California, Berkeley, Berkeley Way West, Berkeley, CA 94720, USA

²Department of Psychiatry and Human Behavior, University of California, Irvine, 101 The City Drive, Orange, CA 92697, USA

³Molecular Biophysics and Integrated Bioimaging, Lawrence Berkeley National Laboratory, 1 Cyclotron Road, Berkeley, CA 94720, USA

⁴Helen Wills Neuroscience Institute, University of California, Berkeley, 132 Barker Hall, Berkeley, CA 94720, USA

⁵Lead Contact

*Correspondence: mpwalker@berkeley.edu

<https://doi.org/10.1016/j.cub.2020.08.017>

SUMMARY

Experimental sleep-wake disruption in rodents and humans causally modulates β -amyloid ($A\beta$) dynamics (e.g., [1–3]). This leads to the hypothesis that, beyond cross-sectional associations, impaired sleep structure and physiology could represent prospective biomarkers of the speed with which $A\beta$ accumulates over time. Here, we test the hypothesis that initial baseline measures of non-rapid eye movement (NREM) sleep slow-wave activity (SWA) and sleep quality (efficiency) provide future forecasting sensitivity to the rate of $A\beta$ accumulation over subsequent years. A cohort of clinically normal older adults was assessed using objective sleep polysomnography in combination with longitudinal tracking of $A\beta$ accumulation with [¹¹C]PiB positron emission tomography (PET) imaging. Both the proportion of NREM SWA below 1 Hz and the measure of sleep efficiency predicted the speed (slope) of subsequent $A\beta$ deposition over time, and these associations remained robust when taking into account additional cofactors of interest (e.g., age, sex, sleep apnea). Moreover, these measures were specific, such that no other macro- and microphysiological architecture metrics of sleep demonstrated such sensitivity. Our data support the proposal that objective sleep markers could be part of a set of biomarkers that statistically forecast the longitudinal trajectory of cortical $A\beta$ deposition in the human brain. Sleep may therefore represent a potentially affordable, scalable, repeatable, and non-invasive tool for quantifying of $A\beta$ pathological progression, prior to cognitive symptoms of Alzheimer's disease (AD).

RESULTS

In short (and see [STAR Methods](#) for details), the study combined overnight polysomnography recording and repeat positron emission tomography (PET) brain scan assessments of β -amyloid ($A\beta$) ([¹¹C]PiB PET) across multiple years in a longitudinal cohort assessment of clinically normal older adults (described in full in [Table 1](#)).

At the initial baseline assessment, participants received in-laboratory sleep recording using full-head electroencephalogram (EEG) polysomnography (PSG), allowing topographical quantification of slow-wave activity (SWA) and macro-sleep architecture including sleep efficiency, as well as non-rapid eye movement (NREM) and rapid eye movement (REM) sleep stages. The mean Pittsburgh Sleep Quality Index global score was 4.1 ± 2.1 , suggesting that sleep quality was comparable to other healthy older adult cohorts [4–6]. Based on previous cross-sectional work [7, 8], a priori measures of interest were sleep efficiency (total amount of sleep as a percentage of total time in bed) and the proportion of SWA between 0.6 and 1 Hz (prop. < 1 Hz SWA). This proportional measure of SWA separates SWA based on the established physiological distinction between NREM slow oscillations <1 Hz and the delta wave (1–4 Hz) [9]. Due to peak sensitivity to $A\beta$ having

been reported at frontal EEG derivations in cross-sectional investigations [8], SWA analyses focused a priori on the mean of frontal electrodes (F3, Fz, and F4). Associated baseline [¹¹C]PiB PET scans were collected within a mean of 6.1 months of polysomnography (± 7.0), a period of time during which $A\beta$ amounts vary minimally within an individual [10]. Following this initial baseline set of assessments, participants received multiple follow-up [¹¹C]PiB PET scans to measure longitudinal change in $A\beta$ accumulation, with a mean duration of follow-up assessment of 3.7 years (± 2.4) and a mean total number of 2.6 PET scans (range 2–5). A standard global cortical [¹¹C]PiB distribution volume ratio (DVR) was calculated for every PET image, and a linear mixed-effects model was used to derive longitudinal slopes of [¹¹C]PiB DVR change for every subject, providing a measure of rate change in $A\beta$ burden over time ([Figure 1](#)). Two participants who were PiB negative at their baseline PET scan were PiB positive at their final scan, based on a DVR threshold of 1.065 [11].

NREM SWA Physiology and Rate of $A\beta$ Accumulation

First, we tested the hypothesis that prop. <1 Hz SWA at baseline was a predictor of the subsequent rate of $A\beta$ accumulation in the future years ahead.

Table 1. Participant Demographics, [^{11}C]PiB PET, and Sleep Characteristics

Demographics (Baseline, n = 32)	
Age, years	75.5 \pm 4.3
Female, n (%)	23 (72)
Education, years	17.0 \pm 1.5
MMSE	29.0 \pm 1.0
ApoE e4 carriers, n (%)	15 (47)
[^{11}C]PiB PET Scans	
PiB+ at baseline, n (%)	20 (63)
No. of PiB scans (range)	2.6 (2–5)
PiB interval, years	3.7 \pm 2.4
Sleep Characteristics	
TST, min	335.3 \pm 70.9
NREM S1 time, min	29.7 \pm 13.8
NREM S2 time, min	176.4 \pm 59.4
NREM SWS time, min	64.3 \pm 44.6
REM time, min	64.8 \pm 27.5
Sleep-onset latency, min	24.8 \pm 36.9
Persistent-sleep latency, min	37.4 \pm 43.2
WASO, min	110.2 \pm 61.5
Sleep efficiency, %	69.9 \pm 14.8
Apnea-hypopnea index	7.3 \pm 9.4
No. of arousals	48.5 \pm 27.4
Arousal index	8.7 \pm 5.5
PSQI global score	4.1 \pm 2.1

All values are mean \pm SD unless otherwise noted. PiB status was determined based on a global PiB DVR threshold of 1.065 [11]. MMSE, Mini-Mental State Examination; TST, total sleep time; NREM, non-rapid eye movement sleep; SWS, slow-wave sleep; S1/S2, stage 1/stage 2; REM, rapid eye movement sleep; WASO, wake after sleep onset; PSQI, Pittsburgh Sleep Quality Index.

Supportive of the hypothesis, individuals with lower prop. <1 Hz SWA at initial baseline went on to experience a significantly greater subsequent rate of cortical A β accumulation, relative to those with higher initial prop. <1 Hz SWA (Figure 2A; $r = -0.52$, $p = 0.002$). In order to account for covariates and number of PET scans per subject over time, a linear mixed-effects model was implemented, containing main effects of baseline prop. <1 Hz SWA, age, sex, and apnea-hypopnea index and their respective time interactions as predictors, as well as random intercepts for each subject. Using this approach, this same association remained, such that the interaction term between initial prop. <1 Hz SWA and time predicted cortical A β accumulation ($p < 0.001$).

To investigate the frequency specificity of the association between SWA and future A β change, bivariate correlation strength between the rate of A β change measure and EEG spectral power at frontal electrode Fz was investigated across 1 Hz frequency bins between 0.6 and 40 Hz (Figure 2B). Only spectral power within 0.6- to 1-, 2- to 3-, 3- to 4-, 4- to 5-, and 5- to 6-Hz bins was significantly associated with future A β change (all $p < 0.02$), indicating particular sensitivity at the lowest frequency ranges. Consistent with our prior studies [8, 12], the directionality

was specific, with 0.6- to 1-Hz power being negatively related to A β change, whereas power at frequencies greater than 1 Hz was positive in association.

As an additional control analysis, we examined whether a more traditional measure of SWA was predictive of the rate of A β change, specifically total relative SWA 0.8–4.6 Hz [13]. There was not a significant association between total SWA and A β change ($r = -0.24$, $p = 0.18$), demonstrating that specific frequencies hold predictive power rather than a summary SWA measure.

No such predictive significant associations with the rate of A β accumulation were identified in any REM frequency bin (Fz, 1 Hz bins, 0.6–40 Hz: all $r < |0.35|$, $p > 0.05$). This lack of REM sleep relationship suggests that it is within the physiological state of NREM sleep itself, and specifically in the low-frequency EEG domain, wherein robust forecasting of A β accumulation is possible, at least in this population of clinically normal older adults.

In a final control analysis, we explored whether NREM slow wave-spindle coupling strength, a measure previously shown to be associated with greater medial temporal lobe tau burden [12], was sensitive to change in A β . There was no significant association between slow wave-spindle coupling strength and the rate of A β change ($r = 0.20$, $p = 0.28$), adding to previous evidence that this measure is not sensitive to A β .

Confirming previous cross-sectional findings [8, 12], the measure of prop. <1 Hz SWA was also cross-sectionally (and negatively) associated with baseline A β burden ($r = -0.57$, $p < 0.001$) and, as expected, this baseline measure of A β was also significantly associated with A β change ($r = 0.80$, $p < 0.001$).

Therefore, both bivariate correlations and a linear mixed-effects model suggest that the initial electrophysiological quality of NREM SWA (prop. <1 Hz SWA) provided a selective and statistically significant signal predicting the future rate of cortical A β accumulation across subsequent years. A binary visual representation of this relationship is provided in Figure 3A, showing the amount of A β accumulation over time (annual) in those individuals with high relative to low prop. <1 Hz SWA (median prop. <1 Hz SWA split).

Sleep Macroarchitecture and Rate of A β Accumulation

Having examined the sensitivity of electrophysiological NREM sleep quality, we next sought to test the related hypothesis that the macroarchitecture of sleep, specifically the qualitative measure of sleep efficiency, offered similar predictive sensitivity.

Confirming the hypothesis, sleep efficiency marginally predicted future change in A β (Figure 2C; $r = -0.35$, $p = 0.05$). More specifically, individuals with worse initial sleep efficiency at baseline went on to show greater subsequent increase in cortical A β accumulation over time. Beyond this bivariate correlation, a linear mixed-effects model was again implemented in order to account for covariates and differing PET scan numbers across subjects. The model contained main effects of baseline sleep efficiency, age, sex, and apnea-hypopnea index and their respective interactions with time as predictors, and random intercepts for each subject. The interaction term between baseline sleep efficiency and time significantly predicted accumulation of A β in the model ($p < 0.001$). This association is visualized in a comparison of annual A β change in high- and

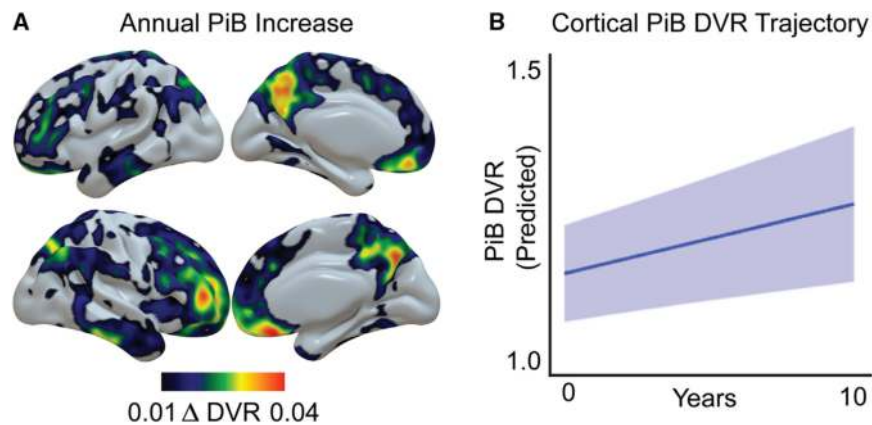


Figure 1. Group-Level Patterns of Longitudinal $[^{11}\text{C}]\text{PiB}$ β -Amyloid Increase

(A) Voxelwise mean group annual $[^{11}\text{C}]\text{PiB}$ DVR increase, highlighting regions of $\text{A}\beta$ plaque accumulation during the study period.

(B) Predicted group longitudinal trajectory of cortical $\text{A}\beta$ plaque deposition (global $[^{11}\text{C}]\text{PiB}$ DVR increase) over time, extracted from a linear mixed-effects model. Light blue shading represents 95% confidence intervals.

low-sleep-efficiency subjects, provided in Figure 3B. Replicating cross-sectional evidence of accelerometer-measured sleep efficiency rather than PSG [7], sleep efficiency was similarly and negatively associated with baseline $\text{A}\beta$ burden ($r = -0.43$, $p = 0.01$).

To examine the specificity of this longitudinal sleep-efficiency relationship, post hoc analyses explored whether other features of baseline sleep macroarchitecture were sensitive in predicting future cortical $\text{A}\beta$ deposition. Baseline total sleep time was negatively correlated with $\text{A}\beta$ change ($r = -0.36$, $p = 0.04$), and wake after sleep onset trended toward a positive correlation ($r = 0.31$, $p = 0.08$), such that shorter sleep duration and greater nighttime wakefulness were associated with a greater rate of $\text{A}\beta$ accumulation. However, neither of these associations survived correction for multiple tests. Nevertheless, the latter two relationships are congruent with the fact that sleep efficiency is calculated from both total amount of sleep and amount of time spent awake during the sleep period. No significant associations were found between other stages of sleep and the rate of $\text{A}\beta$ accumulation (NREM stage 1, $r = 0.07$, $p = 0.72$; NREM stage 2, $r = -0.32$, $p = 0.08$; NREM slow-wave sleep [SWS], $r = -0.07$, $p = 0.72$; REM, $r = -0.18$, $p = 0.34$), indicating specificity to the efficiency of sleep, rather than any specific sleep stage.

Sleep, Rate of $\text{A}\beta$ Accumulation, and Rate of Cognitive Decline

Although the rate of $\text{A}\beta$ accumulation has been linked with declining cognitive function during the same time period [10, 14], $\text{A}\beta$ deposition can occur years in advance of cognitive impairment [15], and does not always predict cognitive status cross-sectionally [16–23]. Nevertheless, we finally sought to examine whether the above measures of sleep that forecasted the rate of $\text{A}\beta$ pathology accumulation were associated with changes in cognition. To do this, slopes of change for memory, working memory, and executive function domain scores from cognitive assessments time locked to $\text{A}\beta$ PET scans were derived.

Decreasing cognitive performance was significant within each domain (one-sample t tests, all $p < 0.001$). We next examined bivariate correlations between baseline prop. <1 Hz SWA and subsequent change in each cognitive domain. Baseline prop. <1 Hz SWA was not significantly associated with change in any of the three cognitive domains (memory, $r = -0.11$,

$p = 0.56$; working memory, $r = 0.10$, $p = 0.61$; executive function, $r = -0.26$, $p = 0.16$). This was also true for the macroarchitecture measure of sleep efficiency with memory ($r = 0.22$, $p = 0.24$), working memory ($r = 0.03$, $p = 0.86$), and executive function ($r = -0.20$, $p = 0.28$). Longitudinal change in $\text{A}\beta$ was negatively correlated with change in the three cognitive domains, although none of the associations were statistically significant (memory, $r = -0.25$, $p = 0.17$; working memory, $r = -0.33$, $p = 0.07$; executive function, $r = -0.12$, $p = 0.52$). This is consistent with reports that $\text{A}\beta$ status in cognitively normal older adults alone is a weak, although at times significant, predictor of cognitive decline [10, 14, 16–23].

In a control analysis, we explored whether NREM slow wave-spindle coupling strength was associated with subsequent changes in cognition. Coupling strength was not predictive of the change in any of the three cognitive domains (memory, $r = -0.15$, $p = 0.42$; working memory, $r = 0.02$, $p = 0.92$; executive function, $r = 0.08$, $p = 0.65$).

Thus, both sleep metrics were sensitive to the rate of $\text{A}\beta$ accumulation over time in cognitively normative older adults, although these same measures were not statistically sensitive in detecting consistent alterations in cognition, the sensitivity of which may only emerge when clinically relevant decline occurs in the years following substantive $\text{A}\beta$ accumulation.

DISCUSSION

Here, we demonstrate that both macro- and microarchitecture features of human sleep are statistically significant predictors of the rate of $\text{A}\beta$ plaque accumulation across subsequent years in cognitively normal older adults. More specifically, worse sleep efficiency and diminished low-frequency <1 Hz slow waves during NREM sleep were associated with the rate of future $\text{A}\beta$ accumulation. These relationships were specific in that no other macroarchitecture features of sleep beyond sleep efficiency, nor spectral frequencies during sleep, demonstrated such significant predictive associations. Furthermore, the associations were robust when taking into account additional factors of interest (e.g., age, sex, and sleep apnea).

Seminal work to date has revealed cross-sectional relationships between sleep disturbance and $\text{A}\beta$ plaque burden measured using PET and cerebrospinal fluid (CSF) [6, 7, 12, 24–27]. Similar cross-sectional association has been identified with slow-wave EEG measures [8, 12, 28, 29]. In addition to the utility of such cross-sectional sensitivity, the ability to forecast subsequent increases in $\text{A}\beta$ is also critical, because the

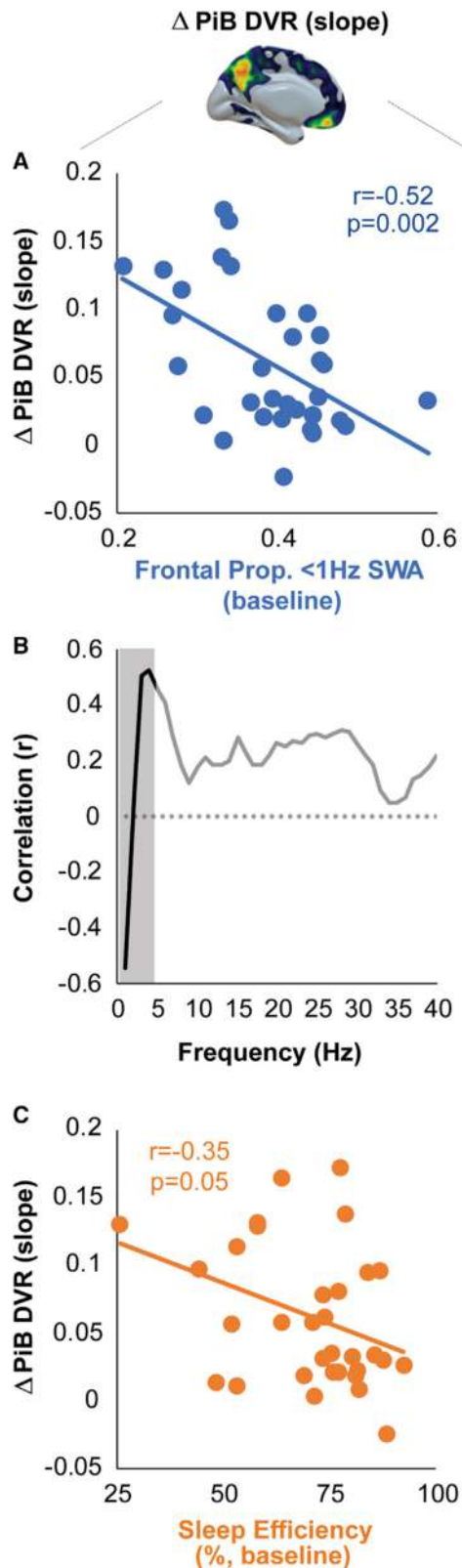


Figure 2. Baseline Sleep Metrics Predict Longitudinal β -Amyloid Plaque Deposition

(A) Scatterplot of significant association between proportion (*prop.*) <1 Hz slow-wave activity (SWA) at baseline and subsequent rate of increase in

rate of increase in $\text{A}\beta$ over time has been associated with the development of subsequent tau pathology, with the downstream consequences of brain atrophy, cognitive decline, and ultimately onset into mild cognitive impairment and Alzheimer's disease (AD) [30–32].

Building on this goal, the current findings demonstrate that measures of human sleep architecture and EEG sleep physiology offer the ability to predict the subsequent rate of $\text{A}\beta$ plaque accumulation. These objective sleep findings complement subjective data demonstrating that self-reported excessive daytime sleepiness [33, 34], as well as features of sleep disordered breathing, specifically obstructive sleep apnea [35, 36], predict greater $\text{A}\beta$ accumulation over time. Therefore, objective measures of nighttime sleep, together with subjective measures of daytime quality of wakefulness, may reflect candidate biomarkers that are non-invasive, safe, relatively cost effective, and sensitive not only to an individual's current $\text{A}\beta$ burden but also to their trajectory of pathological $\text{A}\beta$ progression.

The mechanisms underlying our observed associations may be guided by known causal interactions between sleep and $\text{A}\beta$ dynamics. In rodents, sleep restriction leads to elevations in brain interstitial fluid $\text{A}\beta$ levels, whereas $\text{A}\beta$ plaque pathology increases following chronic sleep deprivation [1, 3]. In humans, both total and selective NREM SWS deprivation result in higher next-day levels of circulating $\text{A}\beta$ in CSF in healthy adults [2, 37, 38], as well as higher $[^{18}\text{F}]\text{florbetaben}$ $\text{A}\beta$ PET signal [39]. The link between the beneficial decrease in CSF $\text{A}\beta$ associated with sleep is thought to be a product of lower synaptic activity during sleep, thereby decreasing synaptic $\text{A}\beta$ release [1] and greater glymphatic brain clearance of extracellular $\text{A}\beta$ during NREM sleep [40, 41].

Adding to this, and of interest from the perspective of AD prevention, rodent work has shown that enhancing cortical slow oscillations through optogenetic stimulation decreases the formation of $\text{A}\beta$ plaques [42]. This may be due to improved regulation of neuronal hyperexcitability that can otherwise elevate $\text{A}\beta$ production [43, 44]. In contrast, driving cortical oscillations at faster frequencies increases $\text{A}\beta$ production and $\text{A}\beta$ plaque deposition [45].

Returning to the current findings, these causal dynamics between sleep and $\text{A}\beta$ may suggest that worse sleep efficiency and impaired NREM slow oscillations could accelerate $\text{A}\beta$ deposition due to elevated synaptic activity driving $\text{A}\beta$ production and/or impair glymphatic clearance of $\text{A}\beta$ over the long term [46]. Supporting the latter possibility is the recent discovery of a genetic link between SWS and astrocytic water channel aquaporin 4 [47].

Whereas the majority of studies to date have reported relationships between NREM sleep and $\text{A}\beta$ dynamics, some findings

cortical $[^{11}\text{C}]\text{PiB}$ DVR. Individuals with lower baseline *prop.* <1 Hz SWA went on to experience higher rates of increase in cortical $\text{A}\beta$ relative to those with higher initial *prop.* <1 Hz SWA.

(B) Correlation between NREM slow-wave sleep (SWS) spectral power in 1 Hz bins (0.6–40 Hz) and subsequent rate of $[^{11}\text{C}]\text{PiB}$ DVR increase. The shaded area represents the a priori SWA frequency range (0.6–4 Hz). The dashed line denotes a correlation of 0.

(C) Scatterplot of bivariate association between baseline sleep efficiency and future rate of $[^{11}\text{C}]\text{PiB}$ DVR increase. Lower sleep efficiency was predictive of a higher rate of increase in cortical $\text{A}\beta$.

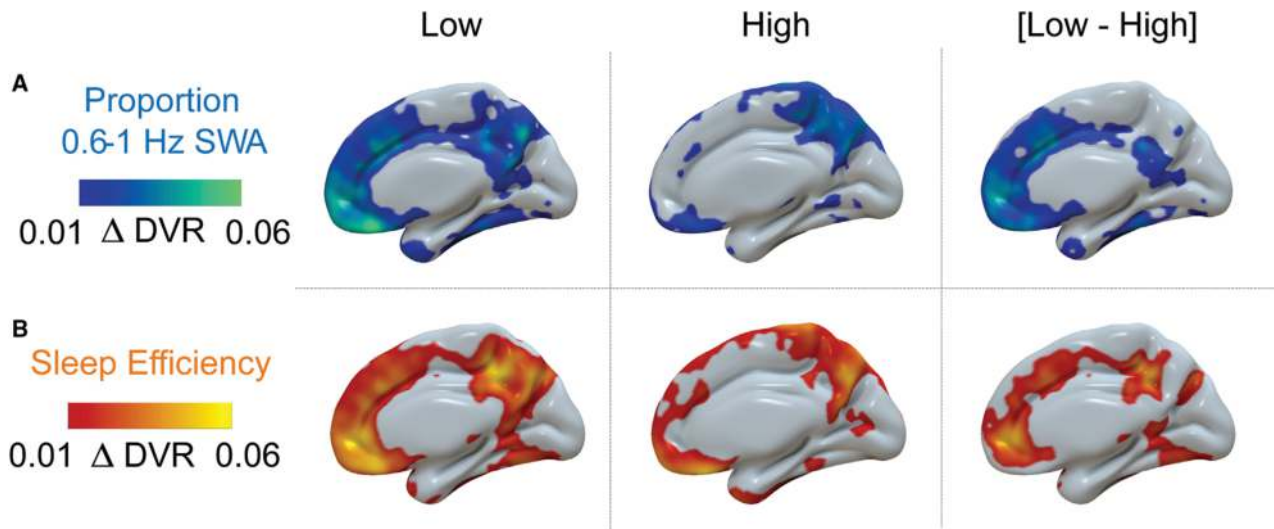


Figure 3. Regional Differences in Patterns of Annual Longitudinal β -Amyloid Accumulation on the Basis of Baseline Sleep Measures

(A) Median split of individuals with high versus low prop. <1 Hz NREM SWA at baseline illustrates distinct patterns of annual [^{11}C]PiB DVR increase, with a greater mean increase in the low prop. <1 Hz SWA group. Far right panel shows voxelwise subtraction of [^{11}C]PiB DVR increase, illustrating the difference between low and high groups.

(B) Median split by baseline sleep efficiency. Mean annual [^{11}C]PiB DVR increase is higher in the low-sleep-efficiency group. All images show the medial surface of the right hemisphere.

have demonstrated associations between REM sleep and $\text{A}\beta$. Cross-sectionally, less time spent in REM sleep is associated with greater brain $\text{A}\beta$, in both rodent models [3] and humans [8, 48]. REM sleep is regulated in part by cholinergic neurons in the basal forebrain [49], subject to neurodegeneration associated with $\text{A}\beta$ burden in AD [50] and providing a potential mechanism explaining this relationship. However, time spent in REM sleep in the current study was not a significant predictor of longitudinal $\text{A}\beta$ increase. This could suggest that age-related pathology that compromises REM sleep is not as strongly associated with longitudinal $\text{A}\beta$ plaque accumulation, at least in this sample of clinically normal older adults.

$\text{A}\beta$ plaque deposition is hypothesized to be an early step in the pathological progression of AD, but relationships between $\text{A}\beta$ and cognition are often weak and can be difficult to detect (e.g., [31, 51]). Consistent with these findings, the sleep measures found to be sensitive to longitudinal $\text{A}\beta$ accumulation in the current study were not predictors of cognitive changes over this same period. It is possible that a robust predictive relationship between these sleep measures and cognition may be observed over a longer period of time or once an individual has transitioned into the stage of mild cognitive impairment or AD. Nevertheless, these results also do not address or preclude the prediction of longitudinal cognitive decline using more detailed episodic memory tests, including those known to be sleep dependent [52]. For example, the impairment of SWA related to $\text{A}\beta$ burden has been shown to impair the overnight consolidation of an episodic memory cross-sectionally [8], and such tasks may show similar associational sensitivity when used longitudinally.

An important and related next step will be to determine whether these objective sleep markers offer similar predictive sensitivity to the rate of $\text{A}\beta$ accumulation in those with mild

cognitive impairment and AD. Considering that impaired sleep is longitudinally predictive of other AD-related outcomes, including gray matter atrophy [53, 54] and later cognitive decline [55–58], this would appear to be an empirically motivated possibility. PET ligands that bind to tau neurofibrillary tangles have only recently been implemented in human research. Greater tau PET signal has been demonstrated to be cross-sectionally associated with disruptions in sleep physiology [12, 28]. As additional longitudinal tau PET data become available, a critical next goal will be to examine the association between sleep and longitudinal changes in tau.

Importantly, the present results cannot establish a causal link between impaired sleep and subsequent $\text{A}\beta$ plaque accumulation. The majority of subjects in the study already had substantial $\text{A}\beta$ deposition at baseline, so the directionality of this relationship cannot be determined without further investigation. Furthermore, our analyses treated PiB DVR as a continuous variable, and were not powered to separate subjects on the basis of initial $\text{A}\beta$ status (positive or negative). By recruiting a large sample of $\text{A}\beta$ -negative subjects, future studies can investigate whether sleep markers hold strength in predicting conversion of $\text{A}\beta$ status from negative to positive. Having established linear relationships between sleep physiology and future $\text{A}\beta$ accumulation, an important next step toward implementing sleep as a diagnostic tool will be to perform large-scale clinical cohort studies that are powered to determine the sensitivity and specificity of these markers through a receiver-operating-characteristic-curve analysis.

Consistent with previous findings [10, 32], $\text{A}\beta$ burden at baseline was strongly associated with the rate of subsequent $\text{A}\beta$ accumulation. To account for this relationship between baseline and rate of subsequent change, we implemented linear mixed-effects models that adjusted for the baseline association by including a random intercept for every subject. These models

demonstrated that prop. <1-Hz SWA and sleep efficiency were significant predictors of change in A β burden over time. A [¹¹C] PIB PET scan is a sensitive marker of the rate of future A β increase [10, 32], yet is costly, invasive, and not widely available. The present findings suggest that sleep assessment could provide a possible non-invasive alternative holding significant predictive strength.

In conclusion, the current data support the hypothesis that objective markers of human sleep are statistically sensitive in forecasting the longitudinal trajectory of cortical A β plaque deposition. Alongside other promising markers [59, 60], the assessment of NREM SWA with EEG, and sleep efficiency measured using EEG or wristwatch actigraphy, could represent part of a set of potentially non-invasive, repeatable, and safe tools for quantification of A β pathological progression, before cognitive symptoms of AD.

Sleep is perhaps unique among other early AD biomarkers in the sense that it not only signals the progression of A β accumulation but is itself a modifiable lifestyle factor. In this regard, further work will need to focus on middle-aged populations prior to substantive A β plaque pathology, thereby determining whether deficits in sleep are detectable prior to A β deposition. This will also be necessary for other AD-related features, such as tau and neurodegeneration. If confirmed, sleep may therefore represent a possible preventative and therapeutic target in modulating risk for AD and/or delaying the onset of AD symptoms.

STAR★METHODS

Detailed methods are provided in the online version of this paper and include the following:

- KEY RESOURCES TABLE
- RESOURCE AVAILABILITY
 - Lead Contact
 - Materials Availability
 - Data and Code Availability
- EXPERIMENTAL MODEL AND SUBJECT DETAILS
 - Participants
- METHOD DETAILS
 - Sleep EEG Acquisition
 - PET Acquisition
 - MRI Acquisition
 - Neuropsychological Evaluation
- QUANTIFICATION AND STATISTICAL ANALYSIS
 - EEG Data
 - PET Processing
 - MRI Processing
 - Statistical analysis

ACKNOWLEDGMENTS

This work was supported by F31AG063428 (to J.R.W.), R01AG031164, RF1AG054019, and RF1AG054106 (to M.P.W.), and R01AG034570 (to W.J.J.) from the National Institutes of Health. We thank the participants of the Berkeley Aging Cohort Study, and Randolph Helfrich, Theresa Harrison, Renaud La Joie, Elizabeth Mormino, Susan Landau, Rachel Bell, Laura Fenton, Kailin Zhuang, Benjamin Miller Mills, and Shai Porat for assistance.

AUTHOR CONTRIBUTIONS

J.R.W., B.A.M., W.J.J., and M.P.W. designed research; J.R.W., B.A.M., S.K., and M.R. performed research; J.R.W., B.A.M., and S.L.B. analyzed data; J.R.W. wrote the first draft of the paper; J.R.W., B.A.M., S.K., M.R., S.L.B., W.J.J., and M.P.W. edited the paper; J.R.W. and M.P.W. wrote the paper.

DECLARATION OF INTERESTS

M.P.W. serves as a consultant for and has equity interest in Bryte, Oura Health Oy, Shuni, and StimScience. W.W.J. serves as a consultant to Genentech, Biogen, Bioclinica, CuraSen, and Grifols. B.A.M. has served as a consultant to Eisai.

Received: May 8, 2020

Revised: July 8, 2020

Accepted: August 5, 2020

Published: September 3, 2020

REFERENCES

1. Kang, J.-E., Lim, M.M., Bateman, R.J., Lee, J.J., Smyth, L.P., Cirrito, J.R., Fujiki, N., Nishino, S., and Holtzman, D.M. (2009). Amyloid-beta dynamics are regulated by orexin and the sleep-wake cycle. *Science* 326, 1005–1007.
2. Lucey, B.P., Hicks, T.J., McLeland, J.S., Toedebusch, C.D., Boyd, J., Elbert, D.L., Patterson, B.W., Baty, J., Morris, J.C., Ovod, V., et al. (2018). Effect of sleep on overnight cerebrospinal fluid amyloid β kinetics. *Ann. Neurol.* 83, 197–204.
3. Roh, J.H., Huang, Y., Bero, A.W., Kasten, T., Stewart, F.R., Bateman, R.J., and Holtzman, D.M. (2012). Disruption of the sleep-wake cycle and diurnal fluctuation of β -amyloid in mice with Alzheimer's disease pathology. *Sci. Transl. Med.* 4, 150ra122.
4. Buysse, D.J., Reynolds, C.F., III, Monk, T.H., Berman, S.R., and Kupfer, D.J. (1989). The Pittsburgh Sleep Quality Index: a new instrument for psychiatric practice and research. *Psychiatry Res.* 28, 193–213.
5. Grandner, M.A., Kripke, D.F., Yoon, I.-Y., and Youngstedt, S.D. (2006). Criterion validity of the Pittsburgh Sleep Quality Index: investigation in a non-clinical sample. *Sleep Biol. Rhythms* 4, 129–139.
6. Brown, B.M., Rainey-Smith, S.R., Villemagne, V.L., Weinborn, M., Bucks, R.S., Sohrabi, H.R., Laws, S.M., Taddei, K., Macaulay, S.L., Ames, D., et al.; AIBL Research Group (2016). The relationship between sleep quality and brain amyloid burden. *Sleep (Basel)* 39, 1063–1068.
7. Ju, Y.-E.S., McLeland, J.S., Toedebusch, C.D., Xiong, C., Fagan, A.M., Duntley, S.P., Morris, J.C., and Holtzman, D.M. (2013). Sleep quality and preclinical Alzheimer disease. *JAMA Neurol.* 70, 587–593.
8. Mander, B.A., Marks, S.M., Vogel, J.W., Rao, V., Lu, B., Saletin, J.M., Ancoli-Israel, S., Jagust, W.J., and Walker, M.P. (2015). β -amyloid disrupts human NREM slow waves and related hippocampus-dependent memory consolidation. *Nat. Neurosci.* 18, 1051–1057.
9. Steriade, M., Nuñez, A., and Amzica, F. (1993). A novel slow (< 1 Hz) oscillation of neocortical neurons in vivo: depolarizing and hyperpolarizing components. *J. Neurosci.* 13, 3252–3265.
10. Villemagne, V.L., Burnham, S., Bourgeat, P., Brown, B., Ellis, K.A., Salvado, O., Szoëke, C., Macaulay, S.L., Martins, R., Maruff, P., et al.; Australian Imaging Biomarkers and Lifestyle (AIBL) Research Group (2013). Amyloid β deposition, neurodegeneration, and cognitive decline in sporadic Alzheimer's disease: a prospective cohort study. *Lancet Neurol.* 12, 357–367.
11. Villeneuve, S., Rabinovici, G.D., Cohn-Sheehy, B.I., Madison, C., Ayakta, N., Ghosh, P.M., La Joie, R., Arthur-Bentil, S.K., Vogel, J.W., Marks, S.M., et al. (2015). Existing Pittsburgh compound-B positron emission tomography thresholds are too high: statistical and pathological evaluation. *Brain* 138, 2020–2033.
12. Winer, J.R., Mander, B.A., Helfrich, R.F., Maass, A., Harrison, T.M., Baker, S.L., Knight, R.T., Jagust, W.J., and Walker, M.P. (2019). Sleep as a

- potential biomarker of tau and β -amyloid burden in the human brain. *J. Neurosci.* **39**, 6315–6324.
- Dijk, D.-J., Hayes, B., and Czeisler, C.A. (1993). Dynamics of electroencephalographic sleep spindles and slow wave activity in men: effect of sleep deprivation. *Brain Res.* **626**, 190–199.
 - Landau, S.M., Horg, A., and Jagust, W.J.; Alzheimer's Disease Neuroimaging Initiative (2018). Memory decline accompanies subthreshold amyloid accumulation. *Neurology* **90**, e1452–e1460.
 - Donohue, M.C., Sperling, R.A., Petersen, R., Sun, C.-K., Weiner, M.W., and Aisen, P.S.; Alzheimer's Disease Neuroimaging Initiative (2017). Association between elevated brain amyloid and subsequent cognitive decline among cognitively normal persons. *JAMA* **317**, 2305–2316.
 - Doraiswamy, P.M., Sperling, R.A., Coleman, R.E., Johnson, K.A., Reiman, E.M., Davis, M.D., Grundman, M., Sabbagh, M.N., Sadowsky, C.H., Fleisher, A.S., et al.; AV45-A11 Study Group (2012). Amyloid- β assessed by florbetapir F 18 PET and 18-month cognitive decline: a multicenter study. *Neurology* **79**, 1636–1644.
 - Farrell, M.E., Kennedy, K.M., Rodrigue, K.M., Wig, G., Bischof, G.N., Rieck, J.R., Chen, X., Festini, S.B., Devous, M.D., Sr., and Park, D.C. (2017). Association of longitudinal cognitive decline with amyloid burden in middle-aged and older adults: evidence for a dose-response relationship. *JAMA Neurol.* **74**, 830–838.
 - Lim, Y.Y., Maruff, P., Pietrzak, R.H., Ames, D., Ellis, K.A., Harrington, K., Lautenschlager, N.T., Szoeke, C., Martins, R.N., Masters, C.L., et al.; AIBL Research Group (2014). Effect of amyloid on memory and non-memory decline from preclinical to clinical Alzheimer's disease. *Brain* **137**, 221–231.
 - Papp, K.V., Mormino, E.C., Amariglio, R.E., Munro, C., Dagley, A., Schultz, A.P., Johnson, K.A., Sperling, R.A., and Rentz, D.M. (2016). Biomarker validation of a decline in semantic processing in preclinical Alzheimer's disease. *Neuropsychology* **30**, 624–630.
 - Resnick, S.M., Sojkova, J., Zhou, Y., An, Y., Ye, W., Holt, D.P., Dannals, R.F., Mathis, C.A., Klunk, W.E., Ferrucci, L., et al. (2010). Longitudinal cognitive decline is associated with fibrillar amyloid-beta measured by [11 C]PiB. *Neurology* **74**, 807–815.
 - Roe, C.M., Fagan, A.M., Grant, E.A., Hassenstab, J., Moulder, K.L., Maue Dreyfus, D., Sutphen, C.L., Benzinger, T.L.S., Mintun, M.A., Holtzman, D.M., and Morris, J.C. (2013). Amyloid imaging and CSF biomarkers in predicting cognitive impairment up to 7.5 years later. *Neurology* **80**, 1784–1791.
 - Snitz, B.E., Weissfeld, L.A., Lopez, O.L., Kuller, L.H., Saxton, J., Singhababu, D.M., Klunk, W.E., Mathis, C.A., Price, J.C., Ives, D.G., et al. (2013). Cognitive trajectories associated with β -amyloid deposition in the oldest-old without dementia. *Neurology* **80**, 1378–1384.
 - Wirth, M., Oh, H., Mormino, E.C., Markley, C., Landau, S.M., and Jagust, W.J. (2013). The effect of amyloid β on cognitive decline is modulated by neural integrity in cognitively normal elderly. *Alzheimers Dement.* **9**, 687–698.e1.
 - Branger, P., Arenaza-Urquijo, E.M., Tomadesso, C., Mézence, F., André, C., de Flores, R., Mutlu, J., de La Sayette, V., Eustache, F., Chételat, G., and Rauchs, G. (2016). Relationships between sleep quality and brain volume, metabolism, and amyloid deposition in late adulthood. *Neurobiol. Aging* **41**, 107–114.
 - Spira, A.P., Gamaldo, A.A., An, Y., Wu, M.N., Simonsick, E.M., Bilgel, M., Zhou, Y., Wong, D.F., Ferrucci, L., and Resnick, S.M. (2013). Self-reported sleep and β -amyloid deposition in community-dwelling older adults. *JAMA Neurol.* **70**, 1537–1543.
 - Sprecher, K.E., Bendlin, B.B., Racine, A.M., Okonkwo, O.C., Christian, B.T., Kosciak, R.L., Sager, M.A., Asthana, S., Johnson, S.C., and Benca, R.M. (2015). Amyloid burden is associated with self-reported sleep in non-demented late middle-aged adults. *Neurobiol. Aging* **36**, 2568–2576.
 - Sprecher, K.E., Kosciak, R.L., Carlsson, C.M., Zetterberg, H., Blennow, K., Okonkwo, O.C., Sager, M.A., Asthana, S., Johnson, S.C., Benca, R.M., and Bendlin, B.B. (2017). Poor sleep is associated with CSF biomarkers of amyloid pathology in cognitively normal adults. *Neurology* **89**, 445–453.
 - Lucey, B.P., McCullough, A., Landsness, E.C., Toedebusch, C.D., McLeland, J.S., Zaza, A.M., Fagan, A.M., McCue, L., Xiong, C., Morris, J.C., et al. (2019). Reduced non-rapid eye movement sleep is associated with tau pathology in early Alzheimer's disease. *Sci. Transl. Med.* **11**, eaa6550.
 - Varga, A.W., Wohlleber, M.E., Giménez, S., Romero, S., Alonso, J.F., Ducca, E.L., Kam, K., Lewis, C., Tanzi, E.B., Tweardy, S., et al. (2016). Reduced slow-wave sleep is associated with high cerebrospinal fluid A β 42 levels in cognitively normal elderly. *Sleep (Basel)* **39**, 2041–2048.
 - Hanseuw, B.J., Betensky, R.A., Jacobs, H.I.L., Schultz, A.P., Sepulcre, J., Becker, J.A., Cosio, D.M.O., Farrell, M., Quiroz, Y.T., Mormino, E.C., et al. (2019). Association of amyloid and tau with cognition in preclinical Alzheimer disease: a longitudinal study. *JAMA Neurol.* **76**, 915–924.
 - Jagust, W. (2018). Imaging the evolution and pathophysiology of Alzheimer disease. *Nat. Rev. Neurosci.* **19**, 687–700.
 - Leal, S.L., Lockhart, S.N., Maass, A., Bell, R.K., and Jagust, W.J. (2018). Subthreshold amyloid predicts tau deposition in aging. *J. Neurosci.* **38**, 4482–4489.
 - Carvalho, D.Z., St Louis, E.K., Knopman, D.S., Boeve, B.F., Lowe, V.J., Roberts, R.O., Mielke, M.M., Przybelski, S.A., Machulda, M.M., Petersen, R.C., et al. (2018). Association of excessive daytime sleepiness with longitudinal β -amyloid accumulation in elderly persons without dementia. *JAMA Neurol.* **75**, 672–680.
 - Spira, A.P., An, Y., Wu, M.N., Owusu, J.T., Simonsick, E.M., Bilgel, M., Ferrucci, L., Wong, D.F., and Resnick, S.M. (2018). Excessive daytime sleepiness and napping in cognitively normal adults: associations with subsequent amyloid deposition measured by PIB PET. *Sleep (Basel)* **41**, zsy152.
 - Bubu, O.M., Pirraglia, E., Andrade, A.G., Sharma, R.A., Gimenez-Badia, S., Umasabor-Bubu, O.Q., Hogan, M.M., Shim, A.M., Mukhtar, F., Sharma, N., et al.; Alzheimer's Disease Neuroimaging Initiative (2019). Obstructive sleep apnea and longitudinal Alzheimer's disease biomarker changes. *Sleep (Basel)* **42**, zsz048.
 - Sharma, R.A., Varga, A.W., Bubu, O.M., Pirraglia, E., Kam, K., Parekh, A., Wohlleber, M., Miller, M.D., Andrade, A., Lewis, C., et al. (2018). Obstructive sleep apnea severity affects amyloid burden in cognitively normal elderly. A longitudinal study. *Am. J. Respir. Crit. Care Med.* **197**, 933–943.
 - Ju, Y.S., Ooms, S.J., Sutphen, C., Macauley, S.L., Zangrilli, M.A., Jerome, G., Fagan, A.M., Mignot, E., Zempel, J.M., Claassen, J.A.H.R., and Holtzman, D.M. (2017). Slow wave sleep disruption increases cerebrospinal fluid amyloid- β levels. *Brain* **140**, 2104–2111.
 - Ooms, S., Overeem, S., Besse, K., Rikkert, M.O., Verbeek, M., and Claassen, J.A.H.R. (2014). Effect of 1 night of total sleep deprivation on cerebrospinal fluid β -amyloid 42 in healthy middle-aged men: a randomized clinical trial. *JAMA Neurol.* **71**, 971–977.
 - Shokri-Kojori, E., Wang, G.-J., Wiers, C.E., Demiral, S.B., Guo, M., Kim, S.W., Lindgren, E., Ramirez, V., Zehra, A., Freeman, C., et al. (2018). β -amyloid accumulation in the human brain after one night of sleep deprivation. *Proc. Natl. Acad. Sci. USA* **115**, 4483–4488.
 - Fultz, N.E., Bonmassar, G., Setsompop, K., Stickgold, R.A., Rosen, B.R., Polimeni, J.R., and Lewis, L.D. (2019). Coupled electrophysiological, hemodynamic, and cerebrospinal fluid oscillations in human sleep. *Science* **366**, 628–631.
 - Xie, L., Kang, H., Xu, Q., Chen, M.J., Liao, Y., Thiyagarajan, M., O'Donnell, J., Christensen, D.J., Nicholson, C., Iliff, J.J., et al. (2013). Sleep drives metabolite clearance from the adult brain. *Science* **342**, 373–377.
 - Kastanenka, K.V., Hou, S.S., Shakerdge, N., Logan, R., Feng, D., Wegmann, S., Chopra, V., Hawkes, J.M., Chen, X., and Bacskai, B.J. (2017). Optogenetic restoration of disrupted slow oscillations halts amyloid deposition and restores calcium homeostasis in an animal model of Alzheimer's disease. *PLoS ONE* **12**, e0170275.
 - Bero, A.W., Yan, P., Roh, J.H., Cirrito, J.R., Stewart, F.R., Raichle, M.E., Lee, J.-M., and Holtzman, D.M. (2011). Neuronal activity regulates the regional vulnerability to amyloid- β deposition. *Nat. Neurosci.* **14**, 750–756.

44. Cirrito, J.R., Yamada, K.A., Finn, M.B., Sloviter, R.S., Bales, K.R., May, P.C., Schoepp, D.D., Paul, S.M., Mennerick, S., and Holtzman, D.M. (2005). Synaptic activity regulates interstitial fluid amyloid-beta levels in vivo. *Neuron* **48**, 913–922.
45. Kastanenka, K.V., Calvo-Rodriguez, M., Hou, S.S., Zhou, H., Takeda, S., Arbel-Ornath, M., Lariviere, A., Lee, Y.F., Kim, A., Hawkes, J.M., et al. (2019). Frequency-dependent exacerbation of Alzheimer's disease neuropathophysiology. *Sci. Rep.* **9**, 8964.
46. Mander, B.A., Winer, J.R., Jagust, W.J., and Walker, M.P. (2016). Sleep: a novel mechanistic pathway, biomarker, and treatment target in the pathology of Alzheimer's disease? *Trends Neurosci.* **39**, 552–566.
47. Ulv Larsen, S.M., Landolt, H.-P., Berger, W., Nedergaard, M., Knudsen, G.M., and Holst, S.C. (2020). Haplotype of the astrocytic water channel AQP4 is associated with slow wave energy regulation in human NREM sleep. *PLoS Biol.* **18**, e3000623.
48. Liguori, C., Romigi, A., Nuccetelli, M., Zannino, S., Sancesario, G., Martorana, A., Albanese, M., Mercuri, N.B., Izzi, F., Bernardini, S., et al. (2014). Orexinergic system dysregulation, sleep impairment, and cognitive decline in Alzheimer disease. *JAMA Neurol.* **71**, 1498–1505.
49. Saper, C.B., Chou, T.C., and Scammell, T.E. (2001). The sleep switch: hypothalamic control of sleep and wakefulness. *Trends Neurosci.* **24**, 726–731.
50. Kerbler, G.M., Fripp, J., Rowe, C.C., Villemagne, V.L., Salvado, O., Rose, S., and Coulson, E.J.; Alzheimer's Disease Neuroimaging Initiative (2014). Basal forebrain atrophy correlates with amyloid β burden in Alzheimer's disease. *Neuroimage Clin.* **7**, 105–113.
51. Jack, C.R., Jr., Knopman, D.S., Jagust, W.J., Petersen, R.C., Weiner, M.W., Aisen, P.S., Shaw, L.M., Vemuri, P., Wiste, H.J., Weigand, S.D., et al. (2013). Tracking pathophysiological processes in Alzheimer's disease: an updated hypothetical model of dynamic biomarkers. *Lancet Neurol.* **12**, 207–216.
52. Klinzing, J.G., Niethard, N., and Born, J. (2019). Mechanisms of systems memory consolidation during sleep. *Nat. Neurosci.* **22**, 1598–1610.
53. Sexton, C.E., Storsve, A.B., Walhovd, K.B., Johansen-Berg, H., and Fjell, A.M. (2014). Poor sleep quality is associated with increased cortical atrophy in community-dwelling adults. *Neurology* **83**, 967–973.
54. Spira, A.P., Gonzalez, C.E., Venkatraman, V.K., Wu, M.N., Pacheco, J., Simonsick, E.M., Ferrucci, L., and Resnick, S.M. (2016). Sleep duration and subsequent cortical thinning in cognitively normal older adults. *Sleep (Basel)* **39**, 1121–1128.
55. Benedict, C., Byberg, L., Cedernaes, J., Hogenkamp, P.S., Giedrat, V., Kilander, L., Lind, L., Lannfelt, L., and Schiöth, H.B. (2015). Self-reported sleep disturbance is associated with Alzheimer's disease risk in men. *Alzheimers Dement.* **11**, 1090–1097.
56. Djonlagic, I., Aeschbach, D., Harrison, S.L., Dean, D., Yaffe, K., Ancoli-Israel, S., Stone, K., and Redline, S. (2019). Associations between quantitative sleep EEG and subsequent cognitive decline in older women. *J. Sleep Res.* **28**, e12666.
57. Lim, A.S.P., Kowgier, M., Yu, L., Buchman, A.S., and Bennett, D.A. (2013). Sleep fragmentation and the risk of incident Alzheimer's disease and cognitive decline in older persons. *Sleep* **36**, 1027–1032.
58. Lysen, T.S., Luik, A.I., Ikram, M.K., Tiemeier, H., and Ikram, M.A. (2020). Actigraphy-estimated sleep and 24-hour activity rhythms and the risk of dementia. *Alzheimers Dement.* Published online June 19, 2020. <https://doi.org/10.1002/alz.12122>.
59. Hadoux, X., Hui, F., Lim, J.K.H., Masters, C.L., Pébay, A., Chevalier, S., Ha, J., Loi, S., Fowler, C.J., Rowe, C., et al. (2019). Non-invasive in vivo hyperspectral imaging of the retina for potential biomarker use in Alzheimer's disease. *Nat. Commun.* **10**, 4227.
60. Thijssen, E.H., La Joie, R., Wolf, A., Strom, A., Wang, P., Iaccarino, L., Bourakova, V., Cobigo, Y., Heuer, H., Spina, S., et al.; Advancing Research and Treatment for Frontotemporal Lobar Degeneration (ARTFL) Investigators (2020). Diagnostic value of plasma phosphorylated tau181 in Alzheimer's disease and frontotemporal lobar degeneration. *Nat. Med.* **26**, 387–397.
61. Jansen, W.J., Ossenkoppele, R., Knol, D.L., Tijms, B.M., Scheltens, P., Verhey, F.R.J., Visser, P.J., Aalten, P., Aarsland, D., Alcolea, D., et al.; Amyloid Biomarker Study Group (2015). Prevalence of cerebral amyloid pathology in persons without dementia: a meta-analysis. *JAMA* **313**, 1924–1938.
62. Folstein, M.F., Folstein, S.E., and McHugh, P.R. (1975). "Mini-mental state": a practical method for grading the cognitive state of patients for the clinician. *J. Psychiatr. Res.* **12**, 189–198.
63. Rechtschaffen, A., and Kales, A. (1968). A Manual of Standardized Terminology, Techniques and Scoring System for Sleep Stages of Human Subjects (Public Health Service, U.S. Government Printing Office).
64. Mathis, C.A., Wang, Y., Holt, D.P., Huang, G.-F., Debnath, M.L., and Klunk, W.E. (2003). Synthesis and evaluation of ^{11}C -labeled 6-substituted 2-arylbenzothiazoles as amyloid imaging agents. *J. Med. Chem.* **46**, 2740–2754.
65. Elman, J.A., Oh, H., Madison, C.M., Baker, S.L., Vogel, J.W., Marks, S.M., Crowley, S., O'Neil, J.P., and Jagust, W.J. (2014). Neural compensation in older people with brain amyloid- β deposition. *Nat. Neurosci.* **17**, 1316–1318.
66. Delis, D.C., Kramer, J.H., Kaplan, E., and Ober, B.A. (2000). California Verbal Learning Test, Second Edition (Psychological Corporation).
67. Wechsler, D. (1997). Wechsler Memory Scale, Third Edition (Psychological Corporation).
68. Smith, A. (1982). Symbol Digit Modalities Test: Manual (Western Psychological Services).
69. Stroop, J.R. (1938). Factors affecting speed in serial verbal reactions. *Psychol. Monogr.* **50**, 38–48.
70. Reitan, R.M., and Wolfson, D. (1985). The Halstead-Reitan Neuropsychological Test Battery: Theory and Clinical Interpretation (Reitan Neuropsychology).
71. Helfrich, R.F., Mander, B.A., Jagust, W.J., Knight, R.T., and Walker, M.P. (2018). Old brains come uncoupled in sleep: slow wave-spindle synchrony, brain atrophy, and forgetting. *Neuron* **97**, 221–230.e4.
72. Mölle, M., Bergmann, T.O., Marshall, L., and Born, J. (2011). Fast and slow spindles during the sleep slow oscillation: disparate coalescence and engagement in memory processing. *Sleep (Basel)* **34**, 1411–1421.
73. Staresina, B.P., Bergmann, T.O., Bonnefond, M., van der Meij, R., Jensen, O., Deuker, L., Elger, C.E., Axmacher, N., and Fell, J. (2015). Hierarchical nesting of slow oscillations, spindles and ripples in the human hippocampus during sleep. *Nat. Neurosci.* **18**, 1679–1686.
74. Dvorak, D., and Fenton, A.A. (2014). Toward a proper estimation of phase-amplitude coupling in neural oscillations. *J. Neurosci. Methods* **225**, 42–56.
75. Logan, J., Fowler, J.S., Volkow, N.D., Wang, G.J., Ding, Y.S., and Alexoff, D.L. (1996). Distribution volume ratios without blood sampling from graphical analysis of PET data. *J. Cereb. Blood Flow Metab.* **16**, 834–840.
76. Price, J.C., Klunk, W.E., Lopresti, B.J., Lu, X., Hoge, J.A., Ziolkowski, S.K., Holt, D.P., Meltzer, C.C., DeKosky, S.T., and Mathis, C.A. (2005). Kinetic modeling of amyloid binding in humans using PET imaging and Pittsburgh compound-B. *J. Cereb. Blood Flow Metab.* **25**, 1528–1547.

STAR★METHODS

KEY RESOURCES TABLE

REAGENT or RESOURCE	SOURCE	IDENTIFIER
Software and Algorithms		
MATLAB 2015a	RRID: SCR_001622	https://www.mathworks.com/products/matlab.html
EEGLAB 13.4.4b	RRID: SCR_007292	https://sccn.ucsd.edu/eeglab/index.php
SPM12	RRID: SCR_007037	http://www.fil.ion.ucl.ac.uk/spm/
FreeSurfer 5.3.0	RRID: SCR_001847	http://surfer.nmr.mgh.harvard.edu/
R	RRID: SCR_001905	http://www.r-project.org/
R package: lme4	RRID: SCR_015654	https://cran.r-project.org/web/packages/lme4/index.html
R package: lmerTest	RRID: SCR_015656	https://cran.r-project.org/web/packages/lmerTest/index.html
FieldTrip 20161016	RRID: SCR_004849	http://www.fieldtriptoolbox.org/
CircStat 2012	RRID: SCR_016651	https://philippberens.wordpress.com/code/circstats/

RESOURCE AVAILABILITY

Lead Contact

Requests for further information and resources should be directed to, and will be fulfilled by, the lead contact, Matthew Walker (mpwalker@berkeley.edu).

Materials Availability

This study did not generate new unique reagents.

Data and Code Availability

Publicly available software and algorithms used for analyses is listed in the [Key Resources Table](#). Data and code used in this study will be shared by application request from a qualified investigator at an academic institute, subject to the negotiation and decision of a university review and data use agreement process.

EXPERIMENTAL MODEL AND SUBJECT DETAILS

Participants

Thirty-two cognitively normal older adults (mean \pm SD age 75.5 \pm 4.3 years, 23 female, see [Table 1](#)) from the Berkeley Aging Cohort Study (BACS) participated in the study, which was approved by the Institutional Review Boards at University of California, Berkeley and Lawrence Berkeley National Laboratories. All participants providing written informed consent. BACS participants who were PiB+ at their baseline PiB scan were over-recruited for longitudinal PET imaging studies, resulting in a longitudinal imaging sample with a higher prevalence of A β positivity than the general population [61]. Exclusion criteria included presence of neurologic or psychiatric disorders, and current use of hypnotic or antidepressant medications. 7 participants (22%) met criteria for clinically significant obstructive sleep apnea (AHI > 15). Participants were free of depressive symptoms, scored \geq 25 on the Mini Mental State Exam [62], and displayed normal performance on neuropsychological testing (1.5 standard deviations within age, education, and sex adjusted means). Subjects who performed below the 1.5 SD cutoff in one follow-up session remained in the study as we were interested in biomarkers underlying age-related memory decline. Cross-sectional PSG and PiB PET data from 17 participants were included in a previous study of A β and sleep-dependent memory consolidation [8]. Cross-sectional PSG and PiB PET data from 20 participants were included in a previous study of A β , tau, and biomarkers of current AD pathological burden [12]. 5 individuals were included in all three studies.

METHOD DETAILS

Sleep EEG Acquisition

All participants abstained from caffeine, alcohol and daytime naps for the 48 hours before and during the study. Participants kept to their habitual sleep-wake rhythms and averaged 7 to 9 hours of reported time in bed per night before study participation, verified by sleep logs.

Polysomnography on the experimental night was recorded using a Grass Technologies Comet XL system (Astro-Med, West Warwick, RI), including 19-channel electroencephalography (EEG) placed using the 10–20 system, including electrooculography (EOG) recorded at the right and left outer canthi (right superior; left inferior) and electromyography (EMG). Reference electrodes were recorded at both the left and right mastoid (A1, A2).

Participants received an adaptation night in the sleep laboratory before the experimental night which additionally included nasal and oral airflow sensors, abdominal and chest belts, and pulse oximetry. Recordings from the adaptation night were used to calculate number of arousals, arousal index, and apnea-hypopnea index, the latter of which was included as a covariate in statistical models. Adaptation night data from one subject were not usable and this subject was excluded from analyses that included apnea-hypopnea index.

Sleep was scored using standard criteria [63] by a single trained scorer (B.A.M.). Sleep scoring was performed blinded to PET data. Sleep onset latency was defined as latency to NREM stage 2. Persistent sleep latency was defined as latency to sleep that persisted for at least 5 mins. Slow wave sleep (SWS) was defined as NREM stages 3–4.

PET Acquisition

^{11}C -PiB was synthesized at the Lawrence Berkeley National Laboratory Biomedical Isotope Facility, using a protocol described in detail previously [64]. ^{11}C -PiB PET imaging was conducted in 3D acquisition mode using either an ECAT EXACT HR scanner (28% of scans) or a BIOGRAPH PET/CT Truepoint 6 scanner (72% of scans; Siemens Medical Systems). Criteria for PiB positivity did not differ between PET scanners used for PiB acquisition, and PiB PET DVR values have been shown not to significantly differ between scanners [65]. Immediately after intravenous injection of approximately 15 mCi of PiB, 90 min of dynamic acquisition frames were obtained (4×15 , 8×30 , 9×60 , 2×180 , 10×300 , and 2×600 s). For each ^{11}C -PiB scan, a 10-minute transmission scan or a CT were obtained for attenuation correction. ^{11}C -PiB PET images were reconstructed using an ordered subset expectation maximization algorithm with weighted attenuation and smoothed with a 4 mm Gaussian kernel with scatter correction.

Baseline ^{11}C -PiB PET scans were collected within 7.9 ± 4.8 months of PSG recordings. Participants had a mean duration of follow-up assessment of 3.7 ± 2.4 years, and a mean total number of 2.6 (range 2–5) PET scans.

MRI Acquisition

In tandem with ^{11}C -PiB PET scans, high-resolution T1-weighted magnetization prepared rapid gradient echo (MPRAGE) images were acquired for every subject on a 1.5T Siemens Magnetom Avanto scanner at LBNL (TR/TE = 2110/3.58 ms, FA = 15° , $1 \times 1 \times 1$ mm resolution).

Neuropsychological Evaluation

31 of 32 subjects had cognitive longitudinal cognitive data available. Neuropsychological data from assessments closest to the baseline ^{11}C -PiB PET scan were used to calculate cognitive composite scores for episodic memory, working memory, and executive function domains. Z scores were calculated as the average of the Z-transformed individual test scores using mean and SD from the first cognitive session data of a larger sample of 225 BACS participants (age: 81.2 ± 7.3 years; education: 16.8 ± 2.1 years; 58% female) that included the participants studied here. The memory composite score comprised short-delay and long-delay (after 20 min) free recall of the California Verbal Learning Test [66] and Visual Reproduction Test [67]. The working memory score included the WMS-III Digit Span test forward and backward total score. The executive function composite score comprised the Digit Symbol test [68], number correct in 60 s in the Stroop Interference Test [69] and “Trail B minus A” score from the Trail Making Test ([70]; score inverted after Z-transformation).

Longitudinal cognitive data had a mean duration of follow-up assessment of 4.2 ± 2.6 years, and a mean total number of 4.3 (range 2–9) assessments. To assess change in cognitive composite scores over time, slopes were generated with linear mixed-effects models for each composite domain in R using the lme4 package.

QUANTIFICATION AND STATISTICAL ANALYSIS

EEG Data

EEG data from the experimental night were imported into EEGLAB and epoched into 5 s bins. Epochs containing artifacts were manually rejected, and the remaining epochs were filtered between 0.4 and 50 Hz. A fast Fourier transform was then applied to the filtered EEG signal at 5 s intervals with 50% overlap and employing Hanning windowing.

A proportional measure of SWA, a measure previously shown to be associated with A β burden [8, 12], was derived by dividing the spectral power between 0.6 and 1 Hz by the sum of spectral power between 0.6 and 4 Hz during NREM SWS [8, 12]. This proportional measure of SWA separates SWA based on the established physiological distinction between NREM slow waves < 1 Hz and the delta

wave (1–4 Hz) [9]. Total SWA was calculated as relative spectral power 0.8–4.6 Hz during NREM SWS [13]. Sleep efficiency was calculated as the total sleep time (TST) divided by total time in bed. For all analyses including SWA, statistical tests were performed *a priori* at the mean of frontal (F3, Fz, F4) electrode derivations, based on previously demonstrated sensitivity to this measure [8, 12].

For control analyses, slow wave–spindle coupling strength during NREM SWS was calculated using a method identical to our previous publications [12, 71]. Event detection of slow oscillations (SOs) and spindles was performed based on previously established algorithms [71–73]. (1) Slow oscillations: the continuous signal was filtered between 0.16 and 1.25 Hz and detected zero crossings. Events were then selected based on time (0.8–2 s duration) and amplitude (75% percentile) criteria. Finally, artifact-free 5 s long segments (± 2.5 s around trough) were extracted from the raw signal. (2) Sleep spindles: the signal was filtered between 12–16 Hz and the analytical amplitude was extracted after applying a Hilbert transform. The amplitude was smoothed with a 200 ms moving average, then thresholded at the 75% percentile (amplitude criterion). Only events that exceeded the threshold for 0.5 to 3 s (time criterion) were accepted. Artifact-free events were then defined as 5 s long sleep–spindle epochs (± 2.5 s), peak-locked. Events were normalized per subject by means of a z-score prior to all subsequent analyses, alleviating power differences between subjects [71]. The mean and standard deviation were derived from the unfiltered event-locked average time course of either SO or spindle events in every participant. Time-frequency representations for artifact-free normalized SO were calculated after applying a 500 ms Hanning window. Spectral estimates (0.5–30 Hz; 0.5 Hz steps) were calculated between -2 and 2 s in steps of 50 ms and baseline-corrected by means of z-score relative to a bootstrapped baseline distribution that was created from all trials (baseline epoch -2 to -1.5 s, 10000 iterations [71]). For event-locked cross-frequency analyses [71, 73, 74], the normalized SO trough-locked data was first filtered into the SO component (0.1–1.25 Hz) and then the instantaneous phase angle was extracted after applying a Hilbert transform. Then the same trials were filtered between 12–16 Hz and the instantaneous amplitude was extracted from the Hilbert transform. Only the time range from -2 to 2 s was considered, to avoid filter edge artifacts. For every subject, channel, and epoch, the maximal sleep spindle amplitude and corresponding SO phase angle were detected. The mean circular direction and resultant vector length across all NREM events were determined using the CircStat toolbox.

PET Processing

^{11}C -PiB data were realigned and frames from the first 20 minutes of acquisition were averaged and coregistered to participants' corresponding structural MRI. Distribution volume ratios (DVRs) for ^{11}C -PiB images were generated with Logan graphical analysis on ^{11}C -PiB frames corresponding to 35–90 min post-injection using a cerebellar gray matter reference region [75, 76]. Cortical ^{11}C -PiB DVR was calculated as a weighted mean across FreeSurfer-derived native space frontal, temporal, parietal, and posterior cingulate cortical regions. Participants were classified as A β -positive if their cortical ^{11}C -PiB DVR was at or above 1.065, a cutoff adapted from previous thresholds developed in our laboratory [11]. To assess change in A β burden over time, linear mixed-effects models were used to generate slopes of cortical ^{11}C -PiB DVR using the lme4 package in R.

In order to visualize voxelwise change in ^{11}C -PiB DVR (Figures 1A and 3), each participant's baseline and final PET images were warped to MNI space, multiplied by an inclusive intracranial mask, and smoothed with a 4mm^3 Gaussian kernel using SPM12. The baseline image was then subtracted from the final image, and the result was divided by the length of the interval between the two images, resulting in a voxelwise annual change in DVR image for each participant.

MRI Processing

T1 MPRAGE scans were processed with FreeSurfer version 5.3.0 to derive ROIs in each subject's native space using the Desikan-Killiany atlas. FreeSurfer ROIs were used to calculate global ^{11}C -PiB PET measures in native space for each subject, as well as the gray matter cerebellum mask used as a reference region in calculating ^{11}C -PiB DVRs.

Statistical analysis

Pearson correlations were used to test for significant bivariate associations between sleep metrics, slope of cortical ^{11}C -PiB DVR, baseline cortical ^{11}C -PiB DVR, and slope of cognitive domain scores. False discovery rate (FDR) correction was used to adjust for testing associations with multiple sleep stages. Linear mixed-effects (LME) models were used to predict repeated-measures of cortical ^{11}C -PiB DVR, with fixed effects of the baseline sleep variable of interest, age, sex, and apnea-hypopnea index, as well as their respective interactions with time, and a random effect for participant intercept.